

Modelling oviduct fluid formation *in vitro*

Short Title

In vitro Derived Oviduct Fluid

Keywords

Oviduct

Fallopian tube

In vitro Derived Oviduct Fluid (*ivDOF*)

Dual culture

Hyperandrogenism

Hypoandrogenism

Authorship

Constantine A. Simintiras^{1*}

Thomas Fröhlich²

Thozhukat Sathyapalan³

Georg Arnold²

Susanne E. Ulbrich⁴

Henry J. Leese¹

Roger G. Sturme¹

Affiliations

¹ Centre for Cardiovascular and Metabolic Research (CCMR), The Hull York Medical School (HYMS), Cottingham Road, Kingston upon Hull, HU6 7RX, UK.

² Ludwig-Maximilian University of Munich, Professor-Huber-Platz 2, Munich, Bavaria, 80539, Germany.

³ The Michael White Centre for Diabetes and Endocrinology, Hull Royal Infirmary (HRI), Hull York Medical School (HYMS), Brocklehurst Building, 220-236 Anlaby Road, Kingston upon Hull, HU3 2RW, UK.

⁴ Swiss Federal Institute of Technology Zurich (ETHZ), Rämistrasse 101, Zürich, 8092, Switzerland.

Abstract

Oviduct fluid is the microenvironment that supports early reproductive processes including fertilisation, embryo cleavage, and genome activation. However, the composition and regulation of this critical environment remains rather poorly defined. This study uses an *in vitro* preparation of the bovine oviduct epithelium, for the novel application of investigating the formation and composition of *in vitro* derived oviduct fluid (*ivDOF*) within a controlled environment. We confirm the presence of oviduct specific glycoprotein 1 in *ivDOF* and show that the amino acid and carbohydrate content resembles that of previously reported *in vivo* data. In parallel, using a different culture system, a panel of oviduct epithelial solute carrier genes, and the corresponding flux of amino acids within *ivDOF* in response to steroid hormones were investigated. The culture system was optimized further to incorporate fibroblasts directly beneath the epithelium. This dual culture arrangement represents more faithfully the *in vivo* environment and impacts on *ivDOF* composition. Lastly, physiological and pathophysiological endocrine states were modelled and their impact on the *in vitro* oviduct preparation evaluated. These experiments help clarify the dynamic function of the oviduct *in vitro* and suggest a number of future research avenues, such as investigating epithelial-fibroblast interactions, probing the molecular aetiologies of subfertility, and optimising embryo culture media.

Introduction

The lumen of the mammalian oviduct can be considered an optimal environment for reproductive processes including fertilisation and early embryo development (Coy *et al* 2012). During this time, critical developmental events occur, including activation of the embryonic genome and fate-decisions of the blastomeres (González *et al* 2011). In the bovine, the early embryo spends approximately 4 days in the oviduct before moving into the uterus (Hackett *et al* 1993). Insights into the dynamic composition, formation, and regulation of oviduct fluid are therefore crucial to our understanding of the early events of mammalian reproduction.

Until now, descriptions of the composition of oviduct fluid have been based on analyses from samples isolated from various species using *in situ* and *ex vivo* techniques (Aguilar & Reyley 2005). These have included oviduct flushes from anaesthetised or slaughtered animals. As discussed by Leese *et al* (2008), these methods are limited and offer narrow scope for experimental exploration. Thus, there is a need for a robust method of studying oviduct fluid within a controlled laboratory environment.

A single layer of epithelial cells provides the limiting barrier between the maternal circulation and the oviduct lumen. In order to examine oviduct fluid formation in detail it is therefore necessary to isolate the oviduct epithelial cells and culture them in a system that maintains their proper spatial relationship as a polarised confluent layer. One method to achieve this is using the Transwell™ system which enables the culture of oviduct epithelia in chambers which allow access to the apical and basal compartments (Walter 1995). This system allows the bidirectional movement of compounds across the oviduct epithelium to be examined. Using such as system, Dickens *et al* (1993) and Cox & Leese (1995) reported that a chloride secreting epithelium sensitive to purinergic agents lined rabbit and bovine oviducts. These findings have been followed up in detail by Keating & Quinlan (2008; 2012). Moreover, the culture of bovine oviduct epithelia on Transwell™ inserts has allowed the basal to apical, and reverse, movement of nutrients across the oviduct epithelium to be examined (Simintiras *et al* 2012).

Building on these early studies, Levanon *et al* (2010) demonstrated that oviduct epithelia could be cultured at an apical-basal air-liquid interface in which the apical chamber was comprised of moist air. Under air-liquid interface conditions, oviduct epithelia resemble the *in vivo* state more closely and can be cultured in this manner long term (Gualtieri *et al* 2012). Interestingly, patches of oviduct epithelial cells maintained at an air-liquid interface for over two weeks post-confluence regained ciliation (Gualtieri *et al* 2013) despite a lack of estradiol supplementation, which is normally required for re-ciliation *in vitro* (Comer *et al* 1998; Ulbrich *et al* 2003). Chen *et al* (2013a) cultured porcine oviduct epithelial cells for more than 10 days at an air-liquid interface together with steroid hormones and found they were morphologically closer to *in vivo* controls. This interesting approach results in a system in which *in vitro* oviduct epithelial cell cultures mimic *in vivo* behaviour more closely.

In spite of these advances, there is only partial knowledge of the mechanisms underlying the formation and regulation of oviduct fluid, especially when compared with epithelia lining tissues such as the gut and the airways. This can be attributed to (a) ethical and technical limitations surrounding the study of oviduct fluid *in vivo*, and (b) the lack of a robust *in vitro* model enabling the exploration of the formation of oviduct fluid, and how the process responds to stimuli under controlled experimental conditions.

We now present a preparation of bovine oviduct epithelial monolayer to perform real time experiments on oviduct fluid formation *in vitro*. With this system, we have confirmed the secretion of OVGP1 protein into the luminal compartment, which comprises a mixture of amino acids whose composition differs from that in the basal compartment. This apical cell-derived fluid is modified following basal supplementation with estradiol, progesterone and testosterone at physiological and pathophysiological concentrations. Furthermore, using a parallel culture system, we have correlated the expression of bovine oviduct epithelial cell (BOEC) solute carrier genes, with the flux of amino acids in *ivDOF*, following hormonal supplementation.

Materials & Methods

Unless stated otherwise, all reagents were sourced from Sigma Aldrich (Dorset, UK).

Bovine Oviduct Epithelial Cell Harvest

Primarily stage II (mid-luteal phase) abattoir-derived bovine reproductive tracts were transported to the laboratory at room temperature in Hank's Buffered Salt Solution (HBSS) (without CaCl₂ and MgCl₂) (Invitrogen), 10 mM HEPES, and 1 µM Aprotinin – although tracts were not staged for experimentation. Tracts reached the laboratory within 90 minutes of slaughter. Cells from isthmus to infundibulum were harvested similarly to Dickens *et al* (1993) and in accordance with the UK Animal and Plant Health Agency (APHA) regulations.

Bovine oviduct epithelial cells (BOECs) and bovine oviduct fibroblast cells (BOFCs) were subsequently isolated based on their differential adhesion times — cells were initially seeded together in T75 flasks (Sarstedt) and following 18 hours of culture, un-adhered BOECs were removed (Cronin *et al* 2012) and re-cultured. Culture medium consisted of 1:1 DMEM and F12; supplemented with 265 U·ml⁻¹ PenStrep, 20 µg·ml⁻¹ Amphotericin B, 2 mM L-Glutamine, 2.5% v/v NCS, 2.5% v/v FBS, and 0.75% w/v BSA.

Bovine Oviduct Epithelial Cell Transwell™ Culture

BOECs were seeded directly onto the apical surface of 24 mm Corning Transwell™ 0.4 µm pore cell culture inserts coated with 10 µg/ml laminin at a density of 10⁶ cells/ml/insert. BOECs were subsequently maintained between apical and basal culture medium-filled chambers, at 39°C in 5% CO₂, 95% air. Apical and basal media were replaced every 48 hours.

Transepithelial Electrochemical Resistance (TEER)

BOEC confluence was determined by Transepithelial Electrochemical Resistance (TEER) measured using an Evom voltmeter fitted with handheld chopstick electrodes

(World Precision Instruments). From cell seeding to reaching full confluence, TEER rose from $250 \Omega \cdot \text{cm}^{-2}$ to $\sim 800 \Omega \cdot \text{cm}^{-2}$ in the course of ~ 10 days. In addition to assessing monolayer confluence prior to experimentation, TEER was also used as a measure of post-treatment cellular integrity. Unless used as a dependent independent variable, data from BOECs whose TEER fell below $700 \Omega \cdot \text{cm}^{-2}$ were excluded from analysis (Simintiras *et al* 2012).

In vitro Derived Oviduct Fluid (ivDOF)

Once confluent, BOECs were cultured in an apical-basal air-liquid interface (Levanon *et al* 2010) — the basal medium comprised 2 ml of culture medium while the apical compartment comprised moist air in 5% CO_2 . After 24 hours, a thin film of fluid formed in the apical chamber — termed *in vitro* Derived Oviduct Fluid (*ivDOF*) (Figure 1A).

Dual Culture

Bovine oviduct fibroblast cells were harvested by trypsinisation from tissue culture flasks after 5 days in culture. 1×10^6 fibroblast cells were added to the basal surfaces of Transwell™ semi-permeable supports (Figure 1B). Fibroblasts were maintained in this manner for approximately 5 days at which point Transwell™ inserts were reorientated and BOECs introduced to the apical surfaces.

Hormonal Supplementation

Hormone stocks were prepared in ethanol prior to supplementation to the basal Transwell™ chamber. Singular steroid hormone concentrations were based on peripheral plasma levels in the bovine throughout the oestrous cycle as previously reported (Kanchev *et al* 1976). Combinatorial stocks to determine the effects of a physiologically relevant range of hormone concentrations on the *in vitro* model were similarly prepared to represent a minimum, mean and maximum pathophysiological endocrine profile (Kanchev *et al* 1976; Pastor *et al* 1998; Balen 2004; Di Sarra *et al* 2013; O'Reilly *et al* 2014). The maximum solvent (ethanol) contribution was $<1\%$ (*v/v*) similar to Bromberg & Klibanov (1995) and showed no effect throughout (Table 1).

Fluorescence Activated Cell Sorting (FACS)

BOECs and BOFCs were identified based on positive staining for cytokeratin-18 (CK18) and vimentin primary antibodies (Abcam, Cambridge, UK), respectively (Rottmayer *et al* 2006; Goodpaster *et al* 2008). Samples were analysed on FACSCalibur flow cytometer (Becton Dickinson, Oxford, UK) running CELLQuest software and >10,000 events were counted, similarly to Vince *et al* (2011).

Haematoxylin and Eosin Staining

Confluent BOECs cultured on TranswellTM inserts were manually isolated using a blade. The supports were rinsed three times in pre-equilibrated PBS prior to 5 minute incubation at room temperature in 100% haematoxylin. Cells were then rinsed three times in 18.2 milliQ water and incubated for 5 minutes with 1% eosin. Following further washes, cells were supplemented with HydromountTM (Natural Diagnostics), placed onto microscope slides, and imaged on a Zeiss ApoTome 2 Observer Z1 microscope with a x20 objective lens and an Axiom 506 mono imager coupled with ZEN imaging software.

Transmission Electron Microscopy (TEM)

BOECs fixed in 2.5% glutaraldehyde in 0.1 M sodium cacodylate buffer, post-fixed in 1% osmium tetroxide in the same buffer, were stained en-bloc in 1% uranyl acetate (aq) then serially dehydrated in ethanol before being embedded in Epon-Aradite resin. (All chemicals from Agar Scientific, Stansted, Essex). Subsequently 50nm sections were cut using a diamond knife on a Leica UC6 Ultramicrotome and collected on carbon-coated copper grids (EM Resolutions, Saffron Walden). Images were obtained using an Ultrascan 4000 digital camera (Gatan Inc, Pleasanton, Ca. USA) attached to a Jeol 2011 Transmission Electron Microscope (Jeol UK Ltd, Welwyn Garden City) running at 120 kV.

Generation of anti-Oviduct Specific Glycoprotein (OVGPI) Antibodies

The peptide KMTVTPDGRAETLERRL corresponding to amino acids 521–537

of bovine OVGP1 (UniProtKB - Q28042) was synthesized with a 433A Peptide Synthesizer (Applied Biosystems, Waltham, MA, USA) using Fmoc chemistry (FastMoc Ω previous peak method, as suggested by the manufacturer) and TentaGel SRAM (RAPP Polymere, Tübingen, Germany) resin. To further increase immunogenicity, a proprietary peptide carrier was C-terminally coupled. Peptide cleavage and deprotection was performed by incubation in 92.5% trifluoroacetic acid, 5% triisopropylsilane, and 2.5% water for 1.5 h. The peptide was precipitated and washed with cool tert-butyl methyl ether. Peptides were further purified using reversed-phase chromatography and the correctness of the peptide was confirmed using matrix-assisted laser desorption ionization-time of flight mass spectrometry (4800 series; Applied Biosystems). Murine anti-OVGP1 sera were generated by immunization of female BALB/c mice in time intervals of 3 wk with 100 μ g peptide applied subcutaneously. For the first injection, complete Freund's adjuvant and for the following three injections, incomplete Freund's adjuvant was used. Bleeding was performed 10 d after the fourth injection.

Western Blotting

OVGP1 from both abattoir-derived oviduct fluid and *iv*DOF was qualitatively identified by sodium dodecyl sulphate polyacrylamide gel electrophoresis (SDS-PAGE). Proteins were separated by 10%-18% gradient SDS-PAGE and transferred to polyvinylidene fluoride (PVDF) membranes. PVDF membranes were blocked for 24 hours with 10% milk dissolved in Tris-buffered saline-Tween (0.1%), then incubated at 4°C with the custom mouse anti-OVGP1 primary antibody described above (1:1000) for 24 hours, washed, and subsequently incubated with an anti-mouse horseradish peroxidase (HRP) linked antibody (1:10000) (Cell Signaling Technologies, USA) for 1hr at room temperature. Bands were visualised by enhanced chemiluminescent (ECL) detection.

Osmolarity and Fluorometric Assays

Osmolarity was measured using an Osmomat 030 Osmometer (Gonotec GmbH, Berlin, Germany). Glucose, lactate, and pyruvate were quantified indirectly using enzyme-linked fluorometric assays as described in Leese (1983), Leese & Barton

(1984), Gardner & Leese (1988, 1990), and Guerif *et al* (2013).

High Performance Liquid Chromatography

High Performance Liquid Chromatography (HPLC) was used to measure 18 amino acids as described previously (Humpherson *et al* 2005).

Quantitative Real Time Polymerase Chain Reaction (qRT-PCR)

At confluence, BOECs from T25 flasks were subjected to hormonal supplementation (Table 1) for 24 hours prior to isolation using trypsin. BOECs were washed four times by centrifugation at 1000 x g for 5 mins at 4°C and resuspension in pre-chilled 1 ml phenol red free HBSS. Total RNA was extracted using Trizol reagent and chloroform (Chomczynski & Sacchi 1987). Global cDNA was synthesised by reverse transcription using the High Capacity cDNA Reverse Transcription Kit (Fisher Scientific) in accordance to manufacturer instructions. The concentration (ng/μl) and purity (A260/A280) of cDNA generated was determined using a NanoDrop spectrophotometer. All cDNA was diluted to 1 μg/ml. Three technical PCR replicates were prepared per sample in optical 96 well plates and sealed before being loaded onto a Step-one Real-Time PCR machine (Applied Biosystems) for qPCR. The bovine specific exon spanning primers used are provided in Table 2. To ensure correct product length, melt curves were performed (Giglio *et al* 2003) whilst $\Delta\Delta C_t$ method (Livak & Schmittgen 2001) was used to determine relative expression.

Experimental Design

Retrieved bovine oviduct epithelia were pooled, typically yielding sufficient viable cells to seed 6 Transwell™ inserts. The standard experimental design was to assign 3 Transwell™ membranes for treatment with the dependent experimental variable and the remaining 3 as negative controls. The *iv*DOF obtained from each group was pooled for subsequent analysis. This was defined as a single biological replicate (n=1). Unless otherwise stated n=3 indicates data from three independent abattoir collections and *iv*DOF isolations.

In this study, *in vitro* derived oviduct fluid (*ivDOF*; Figure 1A) from untreated (native) bovine oviduct epithelial cells was analysed (Figure 3: A-D) and compared with previously reported *in vivo* observations. To interrogate the dynamicity of *ivDOF*, its composition following singular cellular hormonal supplementation was analysed (Figure 3F), and the impact of dual culture (Figure 2B) was also examined (Figure 3G). These data are contrasted against native *ivDOF*. This system was subsequently expanded upon to investigate the impact of physiological vs. pathophysiological endocrine stimulation on fluid composition and cellular physiology (Figure 5: D-G). Flasks were seeded in parallel for gene expression studies to complement *ivDOF* findings (Figures 4 and 5A-C).

Statistical Analyses

Statistical analyses were performed using Prism Graphpad 6 software for Apple Macintosh. All statistical analysis were two way analysis of variance (ANOVA) followed by a Holm-Sidak non-parametric *post hoc* analysis.

Results

BOEC and BOFC Isolation

Figures 2A and 2B confirm the epithelial nature of cells in culture in our model. Additionally, over 95% of cells were positive for CK18, (Figure 2C) and over 99% of the BOFC population stained positive for vimentin (Figure 2D).

ivDOF Characterisation

The volume of *ivDOF* from untreated BOECS after a 24h period of culture was $25.2 \pm 4.5 \mu\text{l}$ (Figure 3A) and the mean osmolarity was $297 \pm 12 \text{ mOsm}$ (Figure 3B). Untreated *ivDOF* contained $4.30 \pm 1.18 \text{ mM}$ glucose, $4.70 \pm 0.68 \text{ mM}$ lactate, and $0.83 \pm 0.34 \text{ mM}$ pyruvate (Figure 3C). Qualitative western blots for OVGP1 were performed on oviduct fluid derived from fresh abattoir tissue (Figure 3D) and compared with blots given by *ivDOF* (Figure 3E). These figures confirm OVGP1 presence in both oviduct fluids. However OVGP1 collected from abattoir derived *in vivo* oviduct fluid showed two prominent bands at 80 kDa and 90 kDa whereas OVGP1 identified in *ivDOF* was present at 60 kDa.

Figure 3F shows that the amino acid composition of *ivDOF* from untreated BOECs was distinct from that in the medium provided basally (C) with respect to 6/18 amino acids measured. When E2 was added to the basal compartment (Table 1), asparagine, histidine, glutamine, threonine and tyrosine secretion were decreased whereas the apical accumulation of serine and glycine were elevated compared to native *ivDOF* (Figure 3F). Similarly the addition of P4 (Table 1) increased the apical flux of glutamine, glycine, arginine, alanine, and lysine whilst decreasing histidine and tyrosine secretion (Figure 3F). Interestingly treatment with T (Table 1) significantly decreased the accumulation of 10 amino acids in *ivDOF* relative to native fluid (Figure 3F). Figure 3G shows that culturing BOECs in a dual culture configuration with basally adjacent BOFCs altered the secretion of 7/18 amino acids: asparagine, histidine, threonine, and tyrosine movement decreased while glutamine, arginine, and tryptophan flux increased.

BOEC Gene Expression

OVGP1 and *ESR1* were expressed in flask-cultured cells post harvest and increased following 24 hours of E2 exposure (Figure 4). In addition, a panel of solute carrier genes was analysed (Table 2). In brief, *SLC1A1* and *SLC6A14* were up-regulated in response to T, *SLC38A7* expression increased following E2 exposure, and *SLC7A1* and *SLC38A5* expression was elevated following P4 supplementation. The ethanol vehicle control showed no significant impact on gene expression.

Impact of Pathophysiological Endocrine Supplementation

To further explore the impact of endocrine action on oviduct epithelial cell secretions, and to test the capacity of the model for investigating disease, one physiological, and two pathophysiological ranges of hormones were added to the basal compartment (Table 1); the latter represented hypo- and hyper- androgenism. Figure 5 panels A-C show that hyperandrogenism (HYPER) increased the expression of *ESR1* in flask cultured BOECs whilst reducing *OVGP1* and *ZOI* expression whereas hypoandrogenism (HYPO) decreased the relative expression of all the genes investigated relative to physiological (PHYS). Hyperandrogenism also reduced BOEC TEER following 24 hours (Figure 5D) and caused an increase in the volume of *ivDOF* produced (Figure 5E). Figure 5F shows that hypo and hyper treatments had no significant impact on the carbohydrate composition of *ivDOF*. Lastly hypoandrogenism reduced histidine, glutamine, glycine, threonine, arginine, alanine, and lysine secretion whereas hyperandrogenism reduced histidine and arginine but elevated the apical accumulation of glycine (Figure 5G).

Discussion

We present a novel application for an existing bovine oviduct epithelial cell preparation, which can be used to examine the formation of oviduct fluid *in vitro* under a variety of conditions. A layer of BOECs were grown on Transwell™ membranes (Figure 1A) and were confirmed as confluent by TEER, expressed CK18 (Figure 2C), and displayed a number of morphological features typical of epithelial cells (Figures 2A and 2B). Following culture in an air-liquid interface for 24 hours a film of liquid appeared in the apical chamber, which contained OVGPI protein (Figure 3E) and was biochemically distinct from the culture medium provided basally (Figure 3F). We therefore propose that this constitutes an *in vitro* Derived Oviduct Fluid (*ivDOF*). We furthermore present a method for achieving dual culture *in vitro* (Figure 1B) and show that incorporating basally adjacent fibroblasts into the model also impacts *ivDOF* amino acid composition (Figure 3G). In addition, analogous flask-cultured BOECs expressed the genes *ESR1* and *OVGPI* in an E2 responsive manner (Figure 4). The above were then expanded to test the capacity of this preparation to model pathophysiological endocrine states (Figure 5).

ivDOF Characterisation

The volume of native *ivDOF* produced in 24 hours was found to be $25.2 \pm 11.0 \mu\text{l}$ (Figure 3A); a rate of formation less than the $1.505 \pm 0.291 \mu\text{l}\cdot\text{min}^{-1}$ previously reported *in vivo* by Hugentobler *et al* (2008). The osmolarity of native *ivDOF* however was $297 \pm 12 \text{ mOsm}$ (Figure 4B) which correlates well with both what has been observed *in vivo* $281.0 \pm 2.56 \text{ mOsm}$ (Paisley & Mickelsen 1979) and the 270 - 300 mOsm range of embryo culture media (Sirard & Coenen 2006). Similarly Hugentobler *et al* (2008) investigated the glucose, lactate and pyruvate composition of *in vivo* bovine oviduct. Multiple t-tests between these data and Figure 3C reveals no significant difference between the basic carbohydrate content of *ivDOF* vs *in vivo*.

OVGPI in *ivDOF* was $\sim 60 \text{ kDa}$ (Figure 4E) suggestive of the de-glycosylated form, in contrast to the $\sim 80\text{-}90 \text{ kDa}$ product titrated from abattoir derived oviduct fluid and cell lysates (Figure 4F) (Boice *et al* 1990; Bauersachs *et al* 2004). Abe & Abe (1993) and Sendai *et al* (1994) also reported two OVGPI specific bands in the murine and

bovine at 95 kDa and ~ 55 kDa respectively. This difference is likely due to a lack of post-translational glycosylation, which would impair electrophoretic mobility by up to 25.3 kDa (Unal *et al* 2008). We suspect this is because the culture medium provided is deficient in substrates such as n-acylglucosamine, required for glycosylation.

The amino acid composition of *ivDOF* (Figure 4F) resembled data on cannulated oviducts of anaesthetised heifers (Hugentobler *et al* 2007). However there were some notable differences between the amino acid content of *in vivo* and *in vitro* oviduct fluid. Histidine was significantly more abundant in *ivDOF* than previously recorded levels in the oviduct lumen (Hugentobler *et al* 2007; Guerin *et al* 1995). One possible explanation for this is that histidine, an imidazole, can act as a pH buffer. The *in situ* bovine oviduct pH is 7.6 (Hugentobler *et al* 2004) whereas *in vitro* BOECs were cultured at ~ pH 7.4. Although a small difference in pH the latter represents a 58.5% increase in free H⁺ ions. It could therefore be the case that the native bovine oviduct epithelium secretes histidine to buffer free H⁺ ions and balance *ivDOF* pH. Addition of E2 caused histidine in *ivDOF* to fall and P4 administration further decreased histidine to 159.3 µM; closer to the levels observed previously *in vivo* (Guerin *et al* 1995). The addition of T dramatically reduced histidine secretion from 1071.1 µM to 9.7 µM thus histidine transport appears to be subject to T regulation in addition to E2 and P4.

Glutamine was present in native *ivDOF* at levels very close to those reported *in vivo* (Guerin *et al* 1995 Hugentobler *et al* 2007), yet significantly lower than the concentration in the basal culture medium (Figure 4F). This is one example that the BOEC epithelium *in vitro* forms a highly selective barrier. E2 drastically reduced apical glutamine flux, from 170.0 µM to 5.3 µM whilst T had no impact and P4 markedly increased glutamine content in *ivDOF* to 953.5 µM. This might relate to the importance of glutamine in bovine embryo metabolism (Rieger *et al* 1992). Thus it is unsurprising that P4, the dominant circulatory hormone during pregnancy elevated oviduct glutamine output.

Next BOECs and BOFCs were simultaneously cultured on either side of the same membrane (Figure 1B) to provide a closer to physiological environment for modelling the oviduct epithelium (Fazleabas *et al* 1997). In this dual culture system, the

composition of *ivDOF* was modified; with increased appearance of 3 amino acids and a decrease in 4 (Figure 3G). Again histidine and glycine were brought to levels more comparable to *in vivo*, perhaps suggestive of a compensatory mechanism of oviduct fluid regulation.

Fibroblast-epithelial communication has been extensively studied in the cells of the airways in a variety of species (Parrinello *et al* 2005, Noble 2008, Woodward *et al* 1998, Srisuma *et al* 2010, Ohshima 2009, Chhetri *et al* 2012, Nishioka *et al* 2015, Knight 2001, Sakai & Tager 2013) but fibroblast-epithelial interactions have been investigated to a much lesser extent in the oviduct. However Chen *et al* (2013b) reported a highly differentiated porcine oviduct epithelial phenotype when cultured in fibroblast-conditioned medium.

BOEC Gene Expression

To further understand the amino acid transport the expression of a number of key amino acid transporters were investigated in BOECs cultured in plastic flasks.

Expression of *Slc1a1*, the high affinity L-aspartate excitatory amino acid co-transporter 3 (EAAC3), was increased in response to T (Figure 4C) in agreement with Franklin *et al* (2006). However *Slc1a1* expression did not respond to P4 *in vitro* corresponding to earlier reports that *Slc1a1* expression decreases in the bovine uterine endometrium during the progesterone dependent phase (day 16-20) of ruminant pregnancy (Forde *et al* 2014). Notably as *Slc1a1* expression rose in response to T aspartate transport fell (Figure 3F) suggesting that aspartate flux is not solely a function of *Slc1a1* gene expression.

Expression of *Slc7a1*, the arginine and lysine specific cationic amino acid transporter 1 (CAT1) (Broer 2008) increased in response to P4 supplementation (Figure 4D), as did the accumulation of arginine and lysine in *ivDOF* when BOECs were supplemented with P4 (Figure 3F). P4 similarly up-regulated *Slc38a5* *in vitro* (Figure 4F) corresponding with an increase in alanine and glycine transport as expected (Figure 3F) and further suggesting that amino acid transport in the oviduct is hormonally regulated.

Using this model, we confirm that BOECs *in vitro* express hormonally responsive genes, which correlate with previously reported *in vivo* findings. In most cases the secretion of amino acids in *ivDOF* correlated well with transporter expression.

The Impact of Pathophysiological Endocrine Supplementation

As a proof-of-principle sub-study, the efficacy of the aforementioned *in vitro* oviduct preparation was tested for studying the impact of disease states on the oviduct epithelium and fluid composition. The model was subjected to pathophysiological endocrine stimuli at either end of the androgenic spectrum, in addition to a physiological hormonal balance as a form of control (Table 1).

ESR1 expression (Figure 5A) in flask-cultured BOECs was surprising as it correlated negatively with E2 supplementation, but positively with T addition to culture (Table 1). This, however, could be explained by T having a low affinity for the oestrogen receptor *in vitro* (Rocheffort & Garcia 1976). *OVGP1* expression was highest following physiological hormonal supplementation (Figure 5B) with hypo- and hyperandrogenic treatment similarly decreasing *ZOI* expression relative to physiological (Figure 5C). To investigate the latter from a functional perspective, using the *in vitro* oviduct model described, TEER measurements were taken, as epithelial resistance is proportional to *ZOI* expression (Sultana *et al* 2013). Figure 5D shows that a hyperandrogenic endocrine profile indeed reduced TEER and moreover increased the volume of *ivDOF* produced (Figure 5E). It is tempting to speculate that this *leaky oviduct* phenotype is driven by impaired ER α activity as *ZOI* expression is responsive to E2 (Zeng *et al* 2004) and ER activity (Weihua *et al* 2003), potentially via a miR-191/425 mediated mechanism (Di Leva *et al* 2013). Moreover Liu *et al* (1999) reported that T reduced TEER in the Caco-2 cell line.

Figure 5F shows that pathophysiological endocrine conditions did not affect glucose, lactate, and pyruvate secretion. Moreover these carbohydrate outputs did not differ from those from untreated cells (Figure 3C) despite the known effects of sex hormone mediated anabolism (Miers & Barrett 1998) and the associated heightened energetic demands. In contrast hyperandrogenic treatment had a lesser impact on amino acid

flux regulation than hypoandrogenism. A striking observation was the elevation of arginine following physiological hormonal supplementation (Figure 5G) compared to all other treatments. Given its role in reproduction (Wu *et al* 2009; Wang *et al* 2015) and early embryo metabolism (Sturmey *et al* 2010; Leary 2015), it is unsurprising that this amino acid would appear in *ivDOF*. Such high appearance could be explained by the fact that arginine can be readily synthesised from glutamate via ornithine (Wu 2010). Glycine was also interesting as it was elevated in *ivDOF* following hyperandrogenic incubation (Figure 5G) but reduced following singular T supplementation (Figure 3F), implying that the regulation of glycine flux is not solely T dependent.

Conclusions

We present a method for examining the formation of oviduct fluid under dual culture and a variety of singular, physiological, and pathophysiological endocrine conditions within a controlled environment. This development offers the prospect of modelling the influence of the oestrous cycle (in animals) and the menstrual cycle (in women) with the possibility of using the data on the *ivDOF* generated to optimise embryo culture media.

Declaration of Interests

The authors declare no conflict of interest.

Funding

CA Simintiras was fully funded by a University of Hull studentship and a Hull York Medical School (HYMS) fellowship.

Acknowledgements

The authors would like to thank staff at ABP, York, UK, Dr L Madden (FACS), Mrs A Lowry (TEM) (University of Hull, UK), Dr A Aburima, Prof KM Naseem (WB), and Ms P Sfyri, and Dr A Matsakas (H&E) (Hull York Medical School, UK), in addition to the University of Hull and the Hull York Medical School for funding CA Simintiras and this work.

References

- Abe H, & Abe M 1993 Immunological detection of an oviductal glycoprotein in the rat. *Journal of experimental zoology* **266** 328–335.
- Aguilar J & Reyley M 2005 The uterine tubal fluid: secretion, composition and biological effects. *Animal reproduction science* **2** (2) 91–105.
- Balen A 2004 The pathophysiology of polycystic ovary syndrome: Trying to understand PCOS and its endocrinology. *Clinical Obstetrics and Gynaecology* **18** (5) 685–706.
- Bauersachs S, Rehfeld S, Ulbrich SE, Mallok S, Prella K, Wenigerkind H, Wolf E 2004 Monitoring gene expression changes in bovine oviduct epithelial cells during the oestrous cycle. *Journal of molecular endocrinology* **32** (2) 449–66.
- Boice ML, Geisert RD, Blair RM, Verhage HG 1990 Identification and characterization of bovine oviductal glycoproteins synthesized at estrus. *Biology of Reproduction* **43** 457–465.
- Bröer S 2008 Amino acid transport across mammalian intestinal and renal epithelia. *Physiological reviews* **88** (1) 249–286.
- Bromberg LE & Klibanov AM 1995 Transport of proteins dissolved in organic solvents across biomimetic membranes. *Proceedings of the National Academy of Sciences of the United States of America* **92** 1262–1266.
- Chen S, Einspanier R, Schoen J 2013a *In vitro* mimicking of estrous cycle stages in porcine oviduct epithelium cells: estradiol and progesterone regulate differentiation,

- gene expression, and cellular function. *Biology of reproduction* **89** (3): 54, 1-12.
- Chen S, Einspanier R, Schoen J 2013b Long-term culture of primary porcine oviduct epithelial cells: Validation of a comprehensive *in vitro* model for reproductive science. *Theriogenology* **80** 862-869.
- Chhetri RK, Phillips ZF, Melissa AT, Oldenburg AL 2012 Longitudinal study of mammary epithelial and fibroblast co-cultures using optical coherence tomography reveals morphological hallmarks of pre-malignancy. *Plos One* **7** (11) 1–7.
- Chomczynski P & Sacchi N 1987 Single-step method of RNA isolation by acid guanidinium thiocyanate-phenol-chloroform extraction. *Analytical Biochemistry* **162** (1) 156–159.
- Comer MT, Leese HJ, Southgate J 1998 Induction of a differentiated ciliated cell phenotype in primary cultures of Fallopian tube epithelium. *Human Reproduction* **13** (11) 3114–3120.
- Cox CI & Leese HJ 1995 Effect of purinergic stimulation on intracellular calcium concentration and transepithelial potential difference in cultured bovine oviduct cells. *Biology of Reproduction* **52** 1244–1249.
- Coy P, Garcia-Vazquez FA, Visconti PE, Aviles M 2012 Roles of the oviduct in mammalian fertilisation. *Reproduction* **144** (6) 649–660.
- Cronin JG, Turner ML, Goetze L, Bryant CE, Sheldon IM 2012 Toll-Like Receptor 4 and MYD88-Dependent Signaling Mechanisms of the Innate Immune System Are Essential for the Response to Lipopolysaccharide by Epithelial and Stromal Cells of the Bovine Endometrium. *Biology of Reproduction* **86** (2): 51, 1–9.
- Di Leva G, Piovan C, Gasparini P, Nkankeu A, Taccioli C, Briskin D, Cheung DG, Bolon B, Anderlucci L, Alder H, Nuovo G, Li M, Iorio MV, Galasso M, Ramasamy S, Marcucci G, Perrotti D, Powell KA, Bratasz A, Garofalo M, Nephew KP, Croce CM 2013 Estrogen Mediated-Activation of miR-191/425 Cluster Modulates Tumorigenicity of Breast Cancer Cells Depending on Estrogen Receptor Status. *PLoS Genetics* **9** (3) e1003311.
- Di Sarra D, Tosi F, Bonin C, Fiers T, Kaufman JM, Signori C, Zambotti F, Dall'Alda M, Caruso B, Zanolini ME, Bonora E, Moghetti P 2013 Metabolic Inflexibility Is a Feature of Women With Polycystic Ovary Syndrome and Is Associated With Both Insulin Resistance and Hyperandrogenism. *Journal of Clinical Endocrinology and Metabolism* **98** (6) 2581–2588.
- Dickens CJ, Southgate J, Leese HJ 1993 Use of primary cultures of rabbit oviduct epithelial cells to study the ionic basis of tubal fluid formation. *Journal of Reproduction and Fertility* **98** 603–610.
- Fazleabas AT, Bell SC, Fleming S, Sun J, Lessey BA 1997 Distribution of integrins and the extracellular matrix proteins in the baboon endometrium during the menstrual cycle and early pregnancy. *Biology of reproduction* **56** (2) 348–356.
- Forde N, Simintiras CA, Sturmeier R, Mamo S, Kelly AK, Spencer TE, Bazer FW,

- Lonergan P 2014 Amino acids in the uterine luminal fluid reflects the temporal changes in transporter expression in the endometrium and conceptus during early pregnancy in cattle. *Plos One* **9** (6) e100010.
- Franklin RB, Zou J, Yu Z, Costello LC 2006 EAAC1 is expressed in rat and human prostate epithelial cells; functions as a high-affinity L-aspartate transporter; and is regulated by prolactin and testosterone. *BioMed Central Biochemistry* **7** (10) 1-8.
- Gardner DK & Leese HJ 1988 The role of glucose and pyruvate transport in regulating nutrient utilization by preimplantation embryos. *Development* **104** 423-429.
- Gardner DK & Leese HJ 1990 Concentrations of nutrients in mouse oviduct fluid and their effects on embryo development and metabolism *in vitro*. *Journal of reproduction and fertility* **88** (1) 361–368.
- Gigilio S, Monis PT, Saint CP 2003 Demonstration of preferential binding of SYBR Green I to specific DNA fragments in real-time multiplex PCR. *Nucleic Acids Research* **15** (22) e136.
- Gonzalez S, Ibanez E, Santalo J 2011 Influence of early fate decisions at the two-cell stage on the derivation of mouse embryonic stem cell lines. *Stem Cell Research* **7** 54-65.
- Goodpaster T, Legesse-Miller S, Hameed MR, Aisner SC, Randolph-Habecker J, Collier HA 2008 An immunohistochemical method for identifying fibroblasts in formalin-fixed, paraffin-embedded tissue. *The journal of histochemistry and cytochemistry* **56** (4) 347–358.
- Gualtieri R, Mollo V, Braun S, Barbato V, Fiorentino I, Talevi R 2012 Long-term viability and differentiation of bovine oviductal monolayers: Bidimensional versus three-dimensional culture. *Theriogenology* **78** (7) 1456–1464.
- Gualtieri R, Mollo V, Braun S, Barbato V, Fiorentino I, Talevi R 2013 Bovine oviductal monolayers cultured under three- dimension conditions secrete factors able to release spermatozoa adhering to the tubal reservoir *in vitro*. *Theriogenology* **79** (3) 429–435.
- Guérin P, Gallois E, Croteau S, Revol N, Maurin F, Guillaud J, Menezo Y 1995 Techniques de recolte et aminogrammes des liquides tudaire et folliculaire chez les femelles domestiques. *Revue de Medecine Veterinaire* **146** 805-814.
- Hackett AJ, Durnford R, Mapletoft RJ & Marcus GJ 1993 Location and status of embryos in the genital tract of superovulated cows 4 to 6 days after insemination. *Theriogenology* **40** 1147–1153.
- Hugentobler S, Morris DG, Kane MT, Sreenan JM 2004 *In situ* oviduct and uterine pH in cattle. *Theriogenology* **61** 1419–1427.
- Hugentobler SA, Diskin MG, Leese HJ, Humpherson PG, Watson T, Sreenan JM, Morris DG 2007 Amino acids in oviduct and uterine fluid and blood plasma during the estrous cycle in the bovine. *Molecular Reproduction and Development* **74** 445-

454.

Hugentobler SA, Humpherson PG, Leese HJ, Sreenan JM, Morris DG 2008 Energy substrates in bovine oviduct and uterine fluid and blood plasma during the oestrous cycle. *Molecular Reproduction and Development* **75** 496-503.

Humpherson PG, Leese HJ, Sturmey RG 2005 Amino acid metabolism of the porcine blastocyst. *Theriogenology* **64** (8) 1852–1866.

Ireland JJ, Murphee RL, Coulson PB 1980 Accuracy of predicting stages of bovine estrous cycle by gross appearance of the corpus luteum. *Journal of Dairy Science* **63** (1) 155-60.

Kanchev LN, Dobson H, Ward WR, Fitzpatrick RJ 1976 Concentration of steroids in bovine peripheral plasma during the oestrous cycle and the effect of betamethasone treatment. *Journal of Reproduction and Fertility* **48** (2) 341-345.

Keating N & Quinlan LR 2008 Effect of basolateral adenosine triphosphate on chloride secretion by bovine oviductal epithelium. *Biology of reproduction* **78** (6) 1119–1126.

Keating N & Quinlan LR 2012 Small conductance potassium channels drive ATP-activated chloride secretion in the oviduct. *American journal of physiology cell physiology* **302** (1) C100– C109.

Knight D 2001 Epithelium-fibroblast interactions in response to airway inflammation. *Immunology and Cell Biology* **79** (2) 160–164.

Leary C 2015 The effect of maternal overweight and obesity on the viability and metabolism of human oocytes and early embryos. PhD Thesis. Hull York Medical School.

Leese HJ 1983 Studies on the movement of glucose, pyruvate and lactate into the ampulla and isthmus of the rabbit oviduct. *Quarterly journal of experimental physiology* **68** (1) 89–96.

Leese HJ & Barton AM 1984 Pyruvate and glucose uptake preimplantation embryos. *Journal of Reproduction and Fertility* **72** 9–13.

Leese HJ, Hugentobler SA, Gray SM, Morris DG, Sturmey RG, Whitear SL, Sreenan JM 2008 Female reproductive tract fluids: composition, mechanism of formation and potential role in the developmental origins of health and disease. *Reproduction, Fertility and Development* **20** 1–8.

Levanon K, Ng V, Piao HY, Zhang Y, Chang MC, Roh MH, Kindelberger DW, Hirsch MS, Crum CP, Marto JA, Drapkin R 2010 Primary *ex vivo* cultures of human fallopian tube epithelium as a model for serous ovarian carcinogenesis. *Oncogene* **29** 1103–1113.

Liu DZ, Lecluyse EL, Thakker DR 1999 Dodecylphosphocholine-mediated enhancement of paracellular permeability and cytotoxicity in Caco-2 cell monolayers. *Journal of Pharmaceutical Sciences* **88** (11) 1161–1168.

Livak KJ & Schmittgen TD 2001 Analysis of relative gene expression data using real-time quantitative PCR and the 2-Delta Delta C(T) Method. *Methods* **25** (4) 402–8.

Miers WR & Barrett EJ 1998 The role of insulin and other hormones in the regulation of amino acid and protein metabolism in humans. *Journal of Basic and Clinical Physiology and Pharmacology* **9** (2-4) 235-354.

Nishioka M, Venkatesan N, Dessalle K, Mogas A, Kyoh S, Lin TY, Nair P, Baglole CJ, Eidelman DH, Ludwig MS, Hamid Q 2015 Fibroblast-epithelial cell interactions drive epithelial- mesenchymal transition differently in cells from normal and COPD patients. *Respiratory Research* **16** (1) 72.

Noble PW 2008 Epithelial fibroblast triggering and interactions in pulmonary fibrosis. *European Respiratory Review* **17** (109) 123–129.

O'Reilly MW, Taylor AE, Crabtree NJ, Hughes BA, Capper F, Crowley RK, Stewart PM, Tomlinson JW, Arlt W 2014 Hyperandrogenemia predicts metabolic phenotype in polycystic ovary syndrome: The utility of serum androstenedione. *Journal of Clinical Endocrinology and Metabolism* **99** (3) 1027–1036.

Ohshima M, Yamaguchi Y, Matsumoto N, Micke P, Takenouchi Y, Nishida T, Kato M, Komiyama K, Abiko Y, Ito K, Otsuka K, Kappert K 2010 TGF- β signaling in gingival fibroblast-epithelial interaction. *Journal of dental research* **89** (11) 1315–1321.

Paisley LG & Mickelsen DW 1979 Continuous collection and analysis of bovine oviduct fluid: preliminary results. *Theriogenology* **11** (5) 375-384.

Parrinello S, Coppe JP, Krtolica A, Campisi J 2005 Stromal-epithelial interactions in aging and cancer: senescent fibroblasts alter epithelial cell differentiation. *Journal of Cell Science* **118** 485-496.

Pastor CL, Griffin-Korf ML, Alio JA, Evans WS, Marshall JC 1998 Polycystic ovary syndrome: evidence for reduced sensitivity of the gonadotropin-releasing hormone pulse generator to inhibition by estradiol and progesterone. *The Journal of clinical endocrinology and metabolism* **83** (2) 582–590.

Rieger D, Loskutoff NM, Betteridge KJ 1992 Developmentally related changes in the metabolism of glucose and glutamine by cattle embryos produced and co-cultured *in vitro*. *Journal of reproduction and fertility* **95** (2) 585–595.

Rochefort H & Garcia M 1976 Androgen on the estrogen receptor: I. Binding and *in vivo* nuclear translocation. *Steroids* **28** (4) 549-560.

Rottmayer, R. Ulbrich SE, Kölle S, Prella K, Neumueller C, Sinowatz F, Meyer HHD, Wolf E, Hiendleder S 2006 A bovine oviduct epithelial cell suspension culture system suitable for studying embryo-maternal interactions: Morphological and functional characterization. *Reproduction* **132** (4) 637–648.

Sakai N & Tager AM 2013 Fibrosis of two: Epithelial cell-fibroblast interactions in pulmonary fibrosis. *Biochimica et Biophysica Acta* **1832** (7) 911–921.

- Sendai Y, Abe H, Kikuchi M, Satoh T, Hoshi H 1994 Purification and molecular cloning of bovine oviduct-specific glycoprotein. *Biology of reproduction* **50** (4) 927–934.
- Simintiras CA, Courts FL, Sturmey RG 2012 Genistein transport across the bovine oviduct epithelium. *Reproduction, Fertility and Development* **25** (1) 208–209.
- Sirard MA & Coenen K 2006 *In vitro* maturation and embryo production in cattle. In *Methods in molecular biology - nuclear transfer protocols: cell reprogramming and transgenesis*, vol 348, pp 35–42. Eds PJ Verma and A Trounson. Totowa NJ: Humana.
- Srisuma S, Bhattacharya S, Simon DM, Solleti SK, Tyagi S, Starcher B, Mariani TJ 2010 Fibroblast growth factor receptors control epithelial- mesenchymal interactions necessary for alveolar elastogenesis. *American Journal of Respiratory and Critical Care Medicine* **181** (8) 838–850.
- Sturmey RG, Bermejo-Alvarez P, Gutierrez-Adan A, Rizos D, Leese HJ, Lonergan P 2010 Amino acid metabolism of bovine blastocysts: A biomarker of sex and viability. *Molecular Reproduction and Development* **77** (3) 285–296.
- Sultana R, McBain AJ, O’Neill CA 2013 Strain-dependent augmentation of tight-junction barrier function in human primary epidermal keratinocytes by *lactobacillus* and *bifidobacterium* Lysates. *Applied and Environmental Microbiology* **79** (16) 4887–4894.
- Ulbrich SE, Kettler A, Einspanier R 2003 Expression and localization of estrogen receptor alpha, estrogen receptor beta and progesterone receptor in the bovine oviduct *in vivo* and *in vitro*. *The Journal of steroid biochemistry and molecular biology* **84** (2–3) 279–289.
- Vince RV, Midgley AW, Laden G, Madden LA 2011 The effect of hyperbaric oxygen preconditioning on heat shock protein 72 expression following *in vitro* stress in human monocytes. *Cell Stress and Chaperones* **16** (3) 339–343.
- Walter I 1995 Culture of bovine oviduct epithelial cells (BOEC). *Anatomical Records* **243** (3) 347–356.
- Wang X, Burghardt RC, Romero JJ, Hansen TR, Wu G, Bazer FW 2015 Functional roles of arginine during the peri-implantation period of pregnancy. III: Arginine stimulates proliferation and interferon tau production by ovine trophoctoerm cells via nitric oxide and polyamine-TSC2-MTOR signalling pathways. *Biology of Reproduction* **92** (3) 1–17.
- Weihua Z, Andersson S, Cheng G, Simpson ER, Warner M, Gustafsson JA 2003 Update on estrogen signaling. *FEBS Letters* **546** (1) 17–24.
- Woodward TL, Sia MA, Blaschuk OW, Turner JD, Laird DW 1998 Deficient epithelial-fibroblast heterocellular gap junction communication can be overcome by co-culture with an intermediate cell type but not by E-cadherin transgene expression. *Journal of cell science* **111** (II) 3529–3539.
- Wu G, Bazer FW, Davis TA, Kim SW, Li P, Rhoads JM, Scatterfield MC, Smith SB,

Spencer TE, Yin Y (2009) Arginine metabolism and nutrition in growth, health, and disease. *Amino Acids* **37** (1) 153-168.

Wu G, 2010 Functional amino acids in growth, reproduction, and health. *Advances in Nutrition* **1**: 31-37.

Zeng R, Li X, Gorodeski GI 2004 Estrogen abrogates transcervical tight junctional resistance by acceleration of occludin modulation. *Journal of Clinical Endocrinology and Metabolism* **89** (10) 5145-5155.

Figure and Table Legends

Figure 1 — (A) Schematic representation of the culture system for *in vitro* Derived Oviduct Fluid (*ivDOF*) production. The basal chamber represents the bloodstream whilst the apical represents the oviduct lumen. (B) The technical method and apparatus innovated for seeding fibroblasts to the basal surface of Transwell™ membranes for establishing dual culture. Large Falcon tubes were cut two thirds from the base and the caps removed. The top end of the Falcon tube was manually fastened over the inverted Transwell™ support whilst the cap was placed over the severed end of the tube. This scaffold could then support cell proliferation on the basal surface of the semi-permeable membrane.

Figure 2 — (A) Haematoxylin and eosin stained bovine oviduct epithelial cells cultured to confluence on Transwell™ membranes and imaged at x20 magnification. (B) Transmission electron microscopy image of bovine oviduct epithelia showing the endoplasmic reticulum (ER), Golgi apparatus (GA), intracellular space (ICS), mitochondria (M), microvilli (MV), nucleus (N), plasma membrane (PM), ribosomes (R), a secretory vesicle (SV), and a tight junction (TJ). (C) FACS analysis of cultured BOEC purity showing mouse IgG1 negative control (background noise), anti-Vimentin 1° antibody (BOFC population), and anti-Cytokeratin 18 1° antibody (BOEC population); all in combination with the Alexafluor 488 nm 2° antibody showing in excess of 95% epithelial purity (representative of n=2) at a fluorescence intensity (FLH-1) between $10^3 - 10^4$. (D) FACS analysis of cultured BOFCs showing mouse IgG1 negative control (background noise), anti-cytokeratin 18 1° antibody (BOEC population), and anti-vimentin 1° antibody (BOFC population) in excess of 99% stromal purity (n=1).

Figure 3 — (A) The volume ($n=6 \pm SD$), (B) osmolarity ($n=3 \pm SD$), and (C) carbohydrate content ($n=3 \pm SD$) of *ivDOF* obtained from native (untreated) epithelia. (D-E) Western (protein immuno) blots for OVGP1 from (D) *in vivo* derived oviduct fluid and cell lysates ($n=1$) and (E) native *ivDOF* (representative of $n=4$). Lane 1 was loaded with a staggered 200 kDa HRP-linked biotinylated protein ladder. Lane 2 with 10 mM (16.5 μ l) total protein, lane 3 with 20 mM (33.3 μ l) and lane 4 with 40 mM (66.7 μ l). Lanes 5-8 were loaded with 40 μ l (arbitrary concentrations) of native *ivDOF*. (F) The amino acid composition of *ivDOF* accumulated apically from native (N) BOECs ($n=12 \pm SD$) vs. culture medium (C) supplied basally ($n=3 \pm SD$) vs. *ivDOF* derived from BOECs basally supplemented with 29.37 pM 17 β -oestradiol (E2; $n=6 \pm SD$) vs. *ivDOF* from BOECs treated with 6.36 nM progesterone (P4; $n=4 \pm SD$) vs. *ivDOF* from BOECs basally supplemented with 62.77 pM testosterone (T; $n=3 \pm SD$). (G) The amino acid profile of native *ivDOF* ($n=12 \pm SD$) vs. *ivDOF* from BOECs cultured with BOFCs basally adjacent in the dual culture arrangement ($n=4 \pm SD$). All *ivDOF* accumulated over 24 hours and $a = p \leq 0.0001$, $b = p \leq 0.001$, $c = p \leq 0.01$, and $d = p \leq 0.05$.

Figure 4 — Gene expression profiles of (A) *ESR1*, (B) *Ovgp1*, (C) *Slc1a1*, (D) *Slc7a1*, (E) *Slc38a2*, (F) *Slc38a5*, (G) *Slc38a7* and (H) *Slc6a14* as determined by qRT-PCR ($n=3 \pm SEM$). BOECs were subjected to 62.77 pM testosterone (T), 29.37 pM 17 β -oestradiol (E2), 6.36 nM progesterone (P4), and 0.45% (*v/v*) ethanol (E) as vehicle control – all for 24 hours. Data were normalised to β -actin whilst the impact of treatment on gene expression was calculated relative to native BOECs. **** = $p \leq 0.0001$, *** = $p \leq 0.001$, ** = $p \leq 0.01$, and * = $p \leq 0.05$.

Figure 5 — The effects of hypoandrogenic (HYPO), physiological (PHYS), and hyperandrogenic (HYPER) like endocrine supplementation on (A) *ESR1*, (B) *OVGP1*, and (C) *ZOI* gene expression ($n=3 \pm SEM$). (D) TEER values from BOECs before and after HYPO, PHYS, and HYER exposure in addition to native ($n=3 \pm SD$). One statistically significant difference was determined by paired t-test ($p=0.0214$). (E) Volumes of *ivDOF* from HYPO, PHYS, and HYER treated BOECs ($n=3 \pm SD$). (F) The carbohydrate composition of *ivDOF* from BOECs subjected to HYPO, PHYS, and HYER exposure ($n=3 \pm SD$). (G) The amino acid content of *ivDOF* obtained

from HYPO, PHYS, and HYPER treated cells ($n=3 \pm SD$). All treatment durations were 24 hours. **** = $p \leq 0.0001$, *** = $p \leq 0.001$, ** = $p \leq 0.01$, and * = $p \leq 0.05$.

Table 1 — Concentration of hormones added to bovine oviduct epithelial cells as different treatments.

Table 2 — List of the bovine specific exon spanning primers used. Those marked * were taken from Ulbrich *et al* (2003) whereas primers marked † from Forde *et al* (2014).

Formatted Figure and Table Legends

Figure 1: **(A)** Schematic representation of the culture system for *in vitro* Derived Oviduct Fluid (*iv*DOF) production. The basal chamber represents the bloodstream whilst the apical represents the oviduct lumen.

(B) The technical method and apparatus innovated for seeding fibroblasts to the basal surface of TranswellTM membranes for establishing dual culture. Large Falcon tubes were cut two thirds from the base and the caps removed. The top end of the Falcon tube was manually fastened over the inverted TranswellTM support whilst the cap was placed over the severed end of the tube. This scaffold could then support cell proliferation on the basal surface of the semi-permeable membrane.

Figure 2: **(A)** Haematoxylin and eosin stained bovine oviduct epithelial cells cultured to confluence on TranswellTM membranes and imaged at x20 magnification. **(B)** Transmission electron microscopy image of bovine oviduct epithelia showing the endoplasmic reticulum (ER), Golgi apparatus (GA), intracellular space (ICS), mitochondria (M), microvilli (MV), nucleus (N), plasma membrane (PM), ribosomes (R), a secretory vesicle (SV), and a tight junction (TJ). **(C)** FACS analysis of cultured BOEC purity showing mouse IgG1 negative control (background noise), anti-Vimentin 1° antibody (BOFC population), and anti-Cytokeratin 18 1° antibody (BOEC population); all in combination with the Alexafluor 488 nm 2° antibody showing in excess of 95% epithelial purity (representative of $n=2$) at a fluorescence intensity (FLH-1) between 10^3

– 10⁴. **(D)** FACS analysis of cultured BOFCs showing mouse IgG1 negative control (background noise), anti-cytokeratin 18 1° antibody (BOEC population), and anti-vimentin 1° antibody (BOFC population) in excess of 99% stromal purity (n=1).

Figure 3: **(A)** The volume (n=6 ± SD), **(B)** osmolarity (n=3 ± SD), and **(C)** carbohydrate content (n=3 ± SD) of *iv*DOF obtained from native (untreated) epithelia. **(D-E)** Western (protein immuno) blots for OVGP1 from **(D)** *in vivo* derived oviduct fluid and cell lysates (n=1) and **(E)** native *iv*DOF (representative of n=4). Lane 1 was loaded with a staggered 200 kDa HRP-linked biotinylated protein ladder. Lane 2 with 10 mM (16.5 µl) total protein, lane 3 with 20 mM (33.3 µl) and lane 4 with 40 mM (66.7 µl). Lanes 5-8 were loaded with 40 µl (arbitrary concentrations) of native *iv*DOF. **(F)** The amino acid composition of *iv*DOF accumulated apically from native (N) BOECs (n=12 ± SD) *vs.* culture medium (C) supplied basally (n=3 ± SD) *vs.* *iv*DOF derived from BOECs basally supplemented with 29.37 pM 17β-oestradiol (E2; n=6 ± SD) *vs.* *iv*DOF from BOECs treated with 6.36 nM progesterone (P4; n=4 ± SD) *vs.* *iv*DOF from BOECs basally supplemented with 62.77 pM testosterone (T; n=3 ± SD). **(G)** The amino acid profile of native *iv*DOF (n=12 ± SD) *vs.* *iv*DOF from BOECs cultured with BOFCs basally adjacent in the dual culture arrangement (n=4 ± SD). All *iv*DOF accumulated over 24 hours and a = p ≤ 0.0001, b = p ≤ 0.001, c = p ≤ 0.01, and d = p ≤ 0.05.

Figure 4: Gene expression profiles of **(A)** *ESR1*, **(B)** *Ovvp1*, **(C)** *Slc1a1*, **(D)** *Slc7a1*, **(E)** *Slc38a2*, **(F)** *Slc38a5*, **(G)** *Slc38a7* and **(H)** *Slc6a14* as determined by qRT-PCR (n=3 ± SEM). BOECs were subjected to 62.77 pM testosterone (T), 29.37 pM 17β-oestradiol (E2), 6.36 nM progesterone (P4), and 0.45% (*v/v*) ethanol (E) as vehicle control – all for 24 hours. Data were normalised to β-actin whilst the impact of treatment on gene expression was calculated relative to native BOECs. **** = p ≤ 0.0001, *** = p ≤ 0.001, ** = p ≤ 0.01, and * = p ≤ 0.05.

Figure 5: The effects of hypoandrogenic (HYPO), physiological (PHYS), and hyperandrogenic (HYPER) like endocrine supplementation on **(A)** *ESR1*, **(B)** *OVGP1*, and **(C)** *ZO1* gene expression (n=3 ± SEM). **(D)** TEER values from BOECs before and after HYPO, PHYS, and HYER exposure in addition to native (n=3 ± SD). One statistically significant difference was determined by paired t-test (p=0.0214). **(E)** Volumes of *iv*DOF from HYPO, PHYS, and HYER treated BOECs (n=3 ± SD). **(F)** The carbohydrate composition of *iv*DOF from BOECs subjected to HYPO, PHYS, and HYER exposure (n=3 ± SD). **(G)** The amino acid content of *iv*DOF obtained from HYPO, PHYS, and HYPER treated cells (n=3 ± SD). All treatment durations were 24 hours. **** = p ≤ 0.0001, *** = p ≤ 0.001, ** = p ≤ 0.01, and * = p ≤ 0.05.

Table 1: Concentration of hormones added to bovine oviduct epithelial cells as different treatments.

Table 2: List of the bovine specific exon spanning primers used. Those marked * were taken from Ulbrich *et al* (2003) whereas primers marked † from Forde *et al* (2014).

Figures and Tables

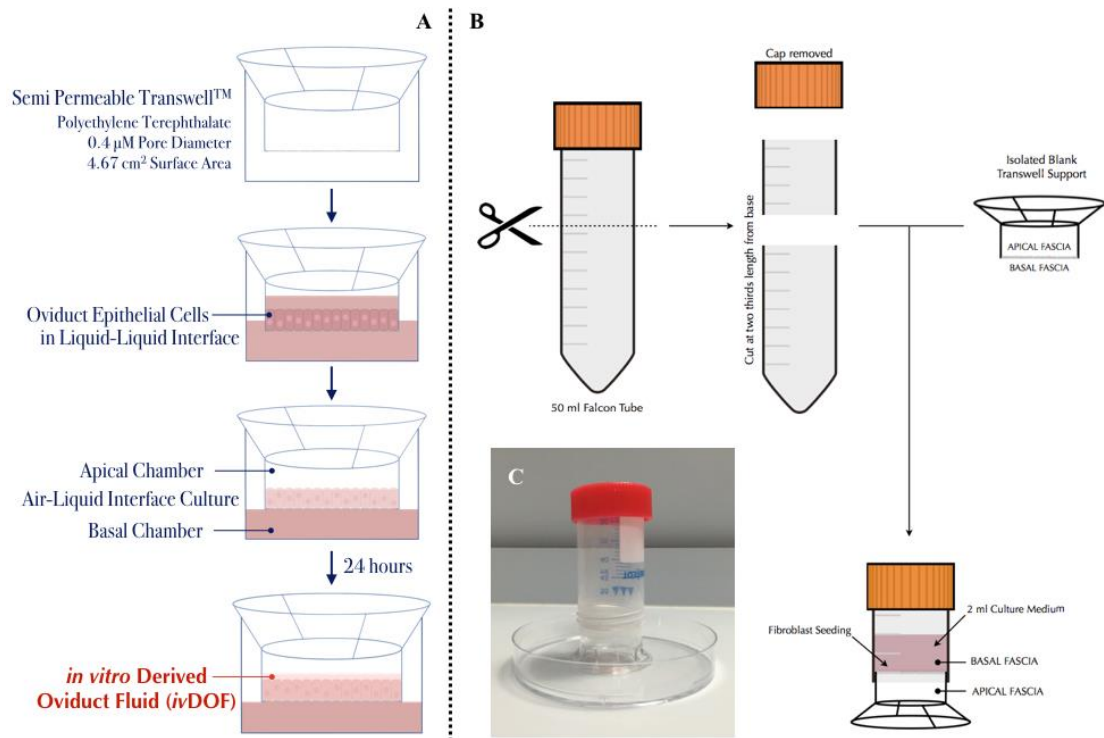


Figure 1

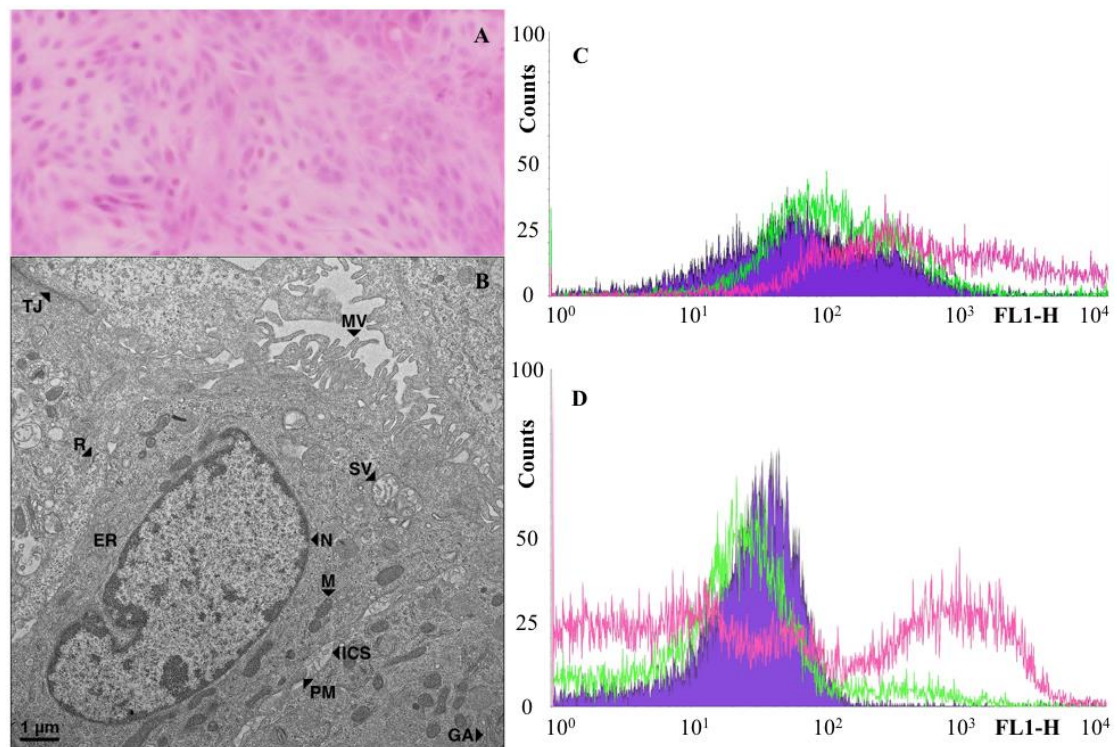


Figure 2

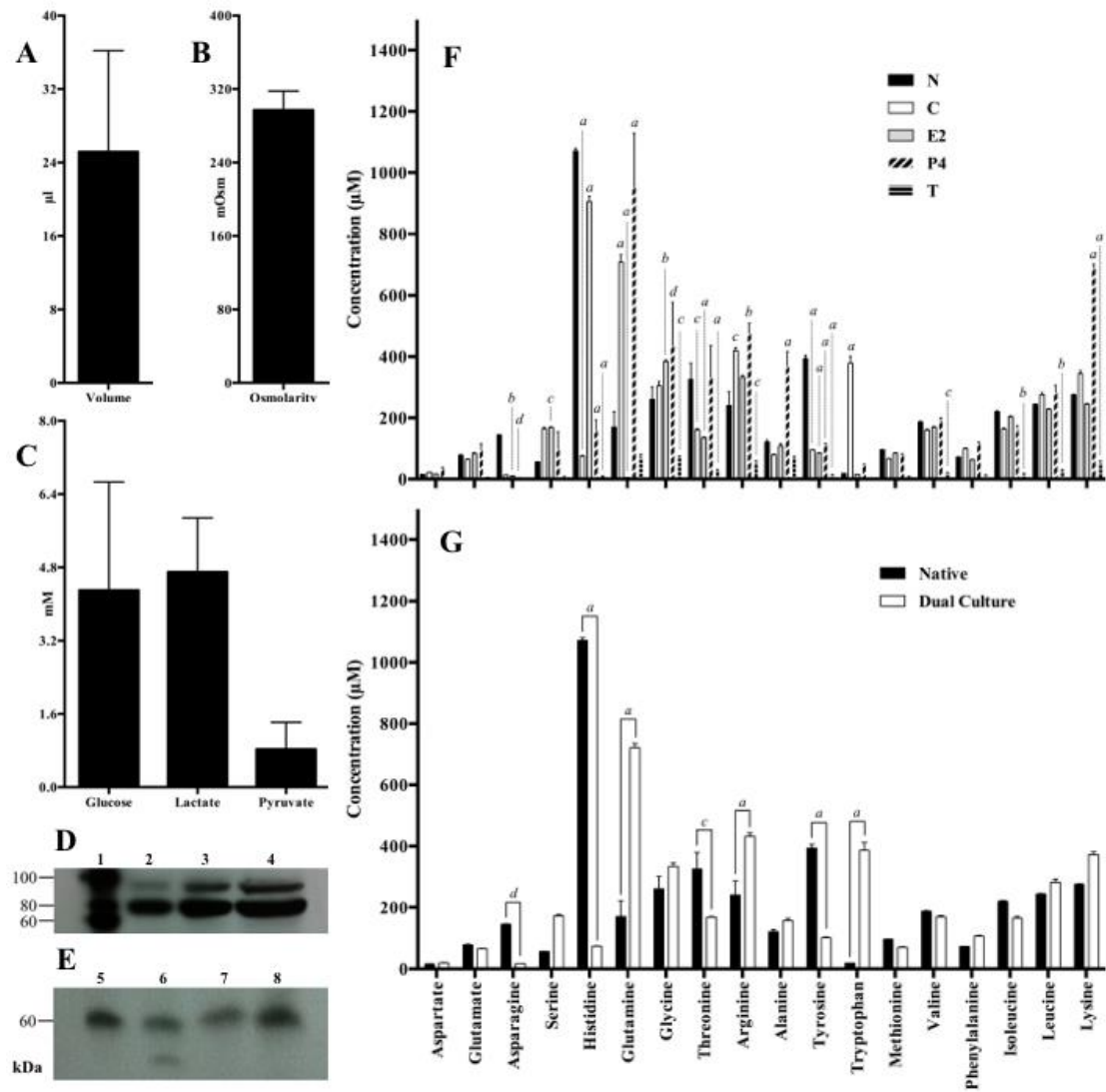


Figure 3

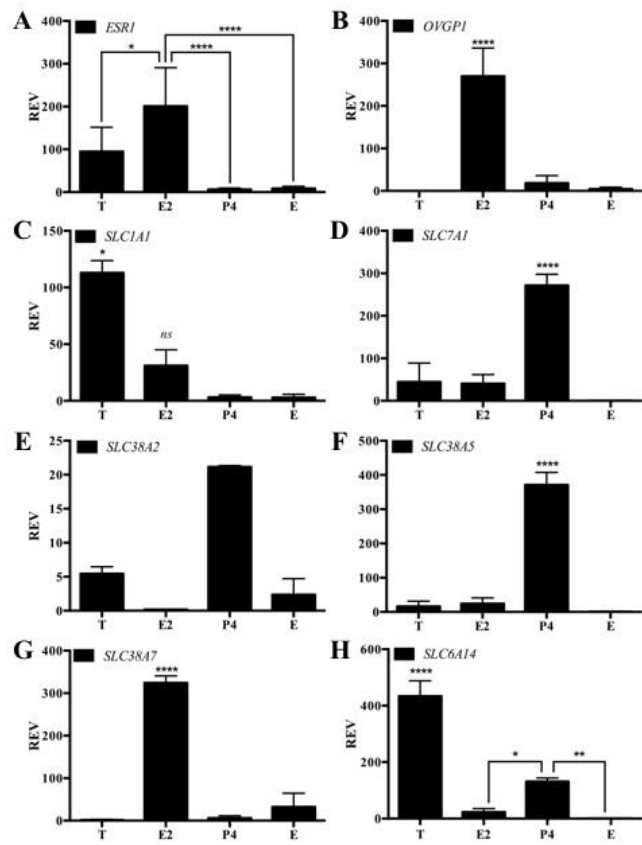


Figure 4

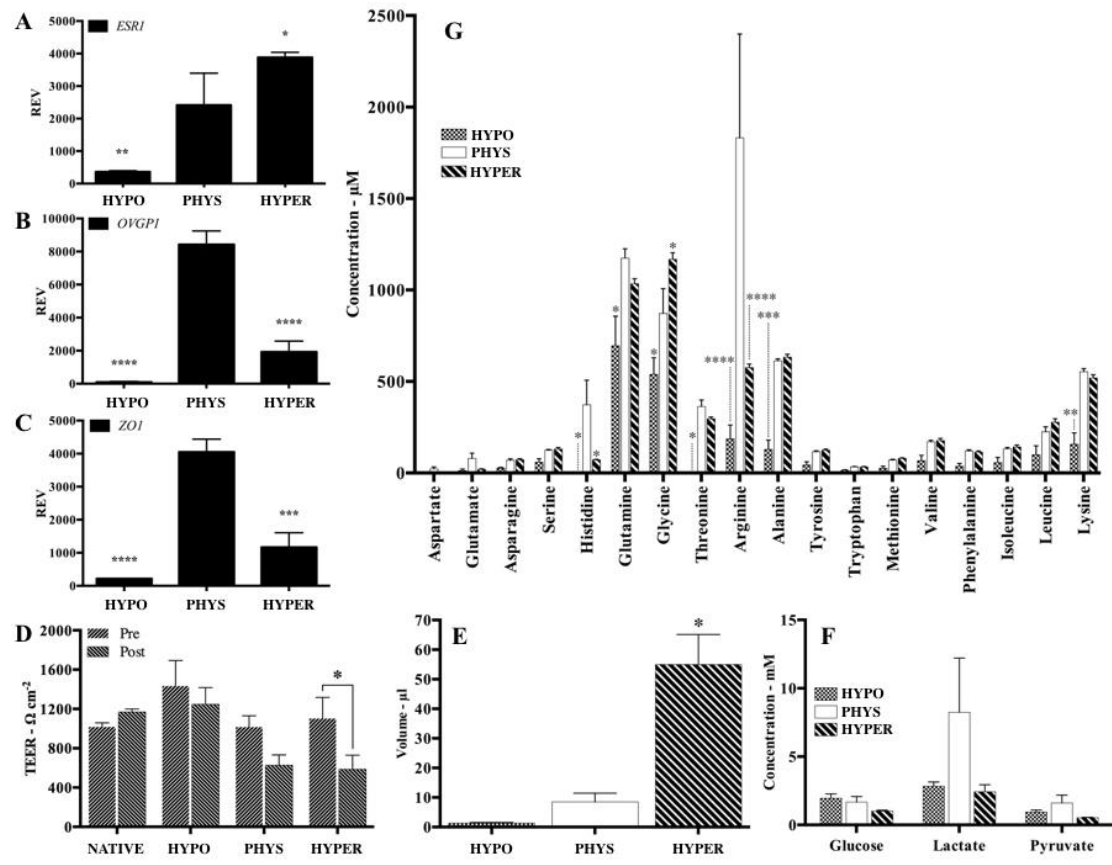


Figure 5

	17β-Oestradiol (E2)	Progesterone (P4)	Testosterone (T)
Native (N)	0 pM	0 pM	0 pM
17β-Oestradiol (E2)	29.37 pM	0 pM	0 pM
Progesterone (P4)	0 pM	6.36 nM	0 pM
Testosterone (T)	0 pM	0 pM	62.77 pM
Hypoandrogenic (HYPO)	29.37 pM	6.36 nM	2.43 pM
Physiological (PHYS)	29.37 pM	6.36 nM	208 pM
Hyperandrogenic (HYPER)	19.46 pM	6.36 nM	6.27 nM

Table 1

Gene	Direction	Sequence	T _m (°C)	GC (%)
<i>β-Actin</i>	Forward (3' to 5')	TTCAACACCCCTGCCATG	59.64	56
	Reverse (5' to 3')	TCACCGGAGTCCATCACGAT	59.73	55
<i>OVGP1</i> *	Forward (3' to 5')	CTGAGCTCCATCCCCACTTG	57.20	60
	Reverse (5' to 3')	GTTGCTCATCGAGGCAAAGG	57.10	55
<i>ESR1</i> *	Forward (3' to 5')	AGGGAAGCTCCTATTTGCTCC	57.00	52
	Reverse (5' to 3')	CGGTGGATGTGGTCCTTCTCT	57.50	57
<i>SLCIA1</i> †	Forward (3' to 5')	CACCGTCCTGAGTGGGCTTGC	61.30	67
	Reverse (5' to 3')	CAGAAGAGCCTGGGCCATTCCC	61.30	64
<i>SLC38A2</i> †	Forward (3' to 5')	GAACCCAGACCACCAAGGCAG	58.10	62
	Reverse (5' to 3')	GTTGGGCAGCGGGAGGAATCG	61.80	67
<i>SLC38A5</i> †	Forward (3' to 5')	TGGCCATCTCGTCTGCTGAGGG	63.20	64
	Reverse (5' to 3')	GCTCCTGCTCCACAGCATTCCC	62.00	64
<i>SLC38A7</i> †	Forward (3' to 5')	CGGCAGCCCGAGGTGAAGAC	61.60	70
	Reverse (5' to 3')	GCCGCAGATACCTGTGCCCAT	60.90	62
<i>SLC6A14</i> †	Forward (3' to 5')	TCGAGGGGCAACTCTGGAAGGT	60.80	59
	Reverse (5' to 3')	GGCAGCATCTTTCCAAACCTCAGCA	62.90	52
<i>ZOI</i>	Forward (3' to 5')	CTCTTCCTGCTTGACCTCCC	56.80	60
	Reverse (5' to 3')	TCCATAGGGAGATTCCCTTCTCA	55.20	45

Table 2